

Microstructural creep damage analysis of induction bent P91 piping in a sodium-cooled fast reactor

Dong-Gi Song^{a*}, Tae-Won Na^a, Jong-Bum Kim^a, Chang-Gyu Park^a, Nak-Hyun Kim^a, June-Hyung Kim^a

^aKorea Atomic Energy Research Institute, Daedeok-daero 989-111, Yuseong-gu, Daejeon, Korea

*Corresponding Author: dgsong@kaeri.re.kr

***Keywords:** Sodium-cooled fast reactor, creep test, induction heating bending pipe, Electron backscatter diffraction

1. Introduction

In a sodium-cooled fast reactor (SFR) system, preventing sodium leakage is crucial due to its high reactivity with air and water [1]. To enhance safety, double-pipe systems are utilized; however, this structure makes it difficult to inspect or repair the internal welds of the pipe. Consequently, minimizing the number of welded joints is crucial to ensure long term reliability and fundamentally reduce potential leakage, which has led to the adoption of induction heating bending technology [2–3].

However, the induction bending process causes pipe thickness variations, specifically thinning at the extrados and thickening at the intrados. Given that SFRs operate under high-temperature conditions over extended periods, it is essential to verify the long-term structural integrity of these induction bent pipes. Therefore, the performance of induction bent pipes should be evaluated under elevated temperatures, particularly through creep testing [4].

In this study, we analyze microstructural creep damage to verify the integrity of induction bent elbows. By comparing the damage characteristics of full-scale elbow specimens with those of rod specimens, a reliable assessment methodology is established for induction bent pipes in SFR applications. The material investigated is P91 (9Cr–1Mo–V) steel, which has good high-temperature properties and corrosion resistance, as listed in the ASME B&PV Code, Sec. III, Div. 5. [2].

2. Methods and Results

The microstructural damage was then analyzed using the electron backscatter diffraction (EBSD) method, which is used to characterize orientation distribution, grain boundary properties, texture index, and the phase distribution of the constituent grains. The EBSD technique provides various quantitative maps and dataset; among these, Kernel average misorientation (KAM) represents the local crystallographic misorientation and is closely correlated with dislocation density and plastic strain distribution. In this study, creep damage was quantitatively evaluated primarily based on KAM values [5].

2.1 Creep damage inspection for creep-tested rod specimens

The rod specimens were extracted from the extrados of an induction bent pipe and subjected to creep testing at 550°C under eight different stress levels: 220, 240, 260, 280, 300, 320, 340, and 360 MPa [6]. Among these, the test for the 220 MPa specimen was interrupted after 1,344 hours because no rupture occurred, whereas creep rupture was observed in all other specimens. Figure 1 presents the fabricated rod specimens alongside a representative image of the creep rupture observed at 360 MPa. For clear specimen identification, Table I lists the labels for the nine tested specimens, including the base material, and summarizes their respective creep rupture times.

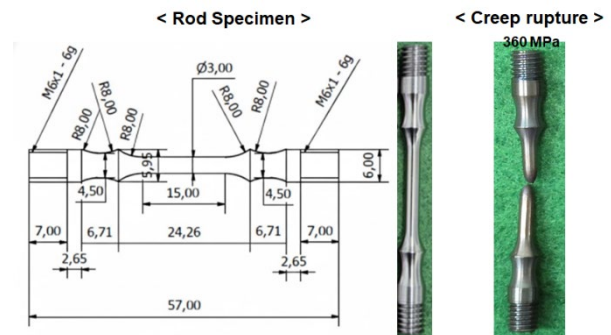


Fig. 1. Schematic illustration and photographs of the fabricated rod specimen, including a representative image of the creep fracture at 360 MPa.

Table I: Identification labels and creep rupture times for the tested P91 specimens.

Label	Load (MPa)	Creep rupture time (hour)
A1 (Base)	–	–
A2	220	–
A3	240	244.9
A4	260	151.3
A5	280	86
A6	300	17.1
A7	320	9.6
A8	340	7.15
A9	360	1.2

To analyze the creep damage precisely, EBSD specimens were extracted from a region within approximately 5 mm of the rupture surface, where the damage was expected to be most concentrated; the center of each extracted sample was then evaluated. Similarly, Specimen A2 (the non-ruptured 220 MPa specimen) was sampled from its mid-section, where damage accumulation was presumed to be most significant. The base material (Specimen A1) was also sampled for reference.

Figure 2 presents a representative KAM map ($50\ \mu\text{m} \times 50\ \mu\text{m}$) of Specimen A9, along with a histogram showing the distribution of misorientation angles. Figure 3 illustrates the average KAM values across all specimens. The results indicate that KAM values increase in correlation with the applied creep stress levels. Notably, the KAM values for the non-ruptured specimens were found to be lower than 0.8041° , which represents the minimum KAM value observed among the ruptured specimens (Specimen A3).

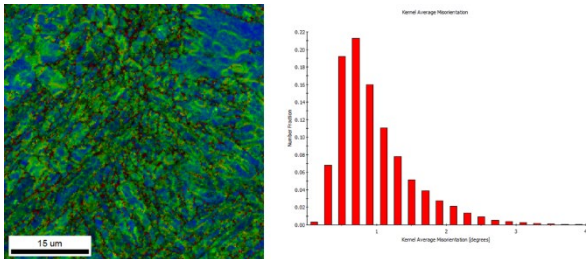


Fig. 2. Representative KAM map ($50\ \mu\text{m} \times 50\ \mu\text{m}$) and the corresponding misorientation angle distribution for Specimen A9.

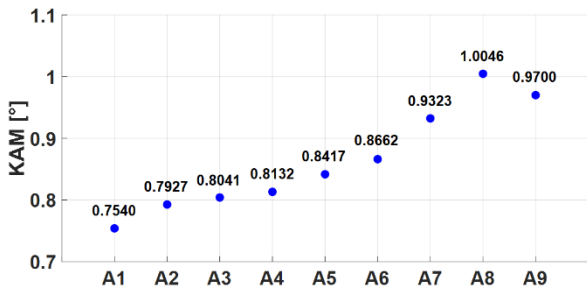


Fig. 3. Average KAM values for the P91 rod specimens under various creep stress levels.

2.2 Creep damage inspection for creep-tested pipes

Creep tests were performed under two distinct conditions: constant stress (referred to as the CREEP1 test) and constant displacement (referred to as the CREEP2 test). The CREEP1 test was conducted at a constant load of 72 kN at 550°C . To ensure equipment safety, the test was terminated after 295 minutes (approximately 5 hours) once the creep deformation exceeded 60 mm, followed by a temperature maintenance period of approximately one hour. The CREEP2 test was performed at 550°C for one month (720 hours) under a fixed displacement corresponding to an initial load of 72 kN [8].

Specimens were extracted from the neutral position, extrados, and intrados at the 45° elbow region, where creep damage was expected to be most concentrated. Additionally, a base material (reference specimen) was sampled from the tangent position, which remained unaffected by the creep load. EBSD analysis was performed at the center of each specimen. Furthermore, as previous studies indicate that load intensity increases toward the inner surface of the pipe, additional analyses were conducted on regions adjacent to the inner surface. [7–8]. Figure 4 illustrates the creep tested pipe, the specific sampling locations, and the measurement regions. Table II provides the specimen labels for identification.

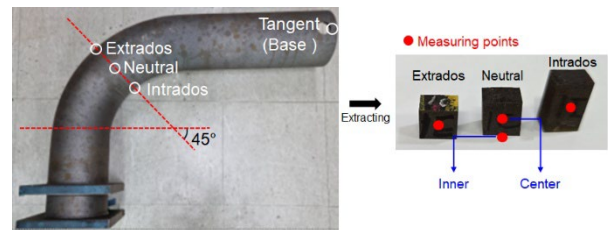


Fig. 4. Schematic of sample extraction locations in the creep-tested pipe and the corresponding measurement regions.

Table II: Labels and descriptions for P91 pipe creep test specimen

Label	Test	Location
C	CREEP1	Tangent (Base)
C1-NC	CREEP1	Neutral-center
C1-NI	CREEP1	Neutral-inner
C1-E	CREEP1	Extrados
C1-I	CREEP1	Intrados
C2-NC	CREEP2	Neutral-center
C2-NI	CREEP2	Neutral-inner
C2-E	CREEP2	Extrados
C2-I	CREEP2	Intrados

Figure 5 presents a representative KAM map ($50\ \mu\text{m} \times 50\ \mu\text{m}$) of the Specimen C1-NI, along with its corresponding misorientation angle distribution histogram. Figure 6 illustrates the average KAM values across the various pipe specimens. The results indicate that KAM values increased in the following order: extrados, intrados, and the neutral position for both the CREEP1 and CREEP2 test conditions. Notably, the inner surface of the neutral position exhibited the highest KAM value among all analyzed locations. This confirms that creep damage was most pronounced near the neutral position and toward the inner surface of the pipe.

Furthermore, the KAM values for all samples from the CREEP1 and CREEP2 tests remained below the threshold of 0.8041° , which represents the minimum value observed at the point of creep rupture in the rod specimens. This comparison indicates that the creep damage accumulated in these pipe samples has not reached the critical level required for rupture, thereby

confirming the structural integrity of the induction bent pipes under the tested creep conditions.

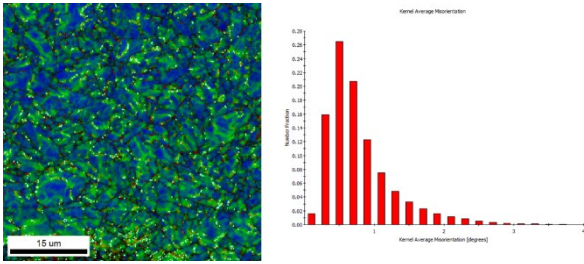


Fig. 5. Representative KAM map (50 $\mu\text{m} \times 50 \mu\text{m}$) and the corresponding misorientation angle distribution for Specimen C1-NI.

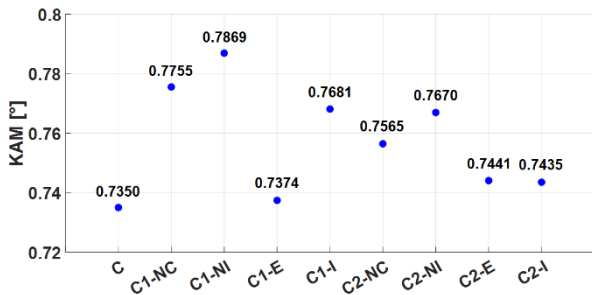


Fig. 6. Comparison of average KAM values for the pipe specimens under CREEP1 and CREEP2 test conditions.

3. Conclusions

In this study, electron backscatter diffraction (EBSD) analysis was performed to evaluate and compare creep damage in P91 steel rod specimens and a full-scale induction bent pipe elbow. The results demonstrated a distinct increase in Kernel average misorientation (KAM) values in correlation with applied stress levels and the duration of creep exposure, confirming that KAM serves as a reliable metric for quantifying creep damage.

In the induction bent pipe, the highest KAM values were observed at the inner surface near the neutral position, identifying this region as the most susceptible to creep induced degradation. Crucially, the KAM values measured across all pipe sections remained consistently below the critical threshold of 0.8041° established from the ruptured rod specimens. These findings provide quantitative evidence confirming the structural integrity of the induction bent piping system under the investigated high-temperature creep conditions

Acknowledgement

This work was supported by a grant from the National Research Foundation of Korea (NRF) funded by the Korean government (Ministry of Science and ICT) (RS-2022-00155157).

REFERENCES

- [1] J. Eoh et al., "Design and safety features of SALUS-100: A long fuel-cycled sodium-cooled fast reactor", Nuclear Engineering and Design, Vol. 420, pp. 112996, 2024.
- [2] T.W. Na, N.H. Kim, C.G. Park, J.H. Kim, I.K. Oh, "Validation of applicability of induction bending process to P91 piping of prototype Gen-IV SFR (PGSFR)", Nuclear Engineering and Technology. 55 (2023) 3571–3580.
- [3] N.H. Kim, et al., "Applicability of the induction bending process to the P91 pipe of the PGSFR", Nuclear Engineering and Technology, Vol. 53 pp.1580–1586, 2021.
- [4] ASTM International, ASTM E139-11: Standard Test Methods for Conducting Creep, Creep-Rupture, and Stress-Rupture Tests of Metallic Materials,
- [5] K. Zhang, et al., "Characterization of geometrically necessary dislocation evolution during creep of P91 steel using electron backscatter diffraction", Materials Characterization, Vol. 195, pp. 112501, 2023.
- [6] T.W. Na et al., "Creep Properties of P91 Induction Bent Pipe for PGSFR", Transactions of the Korean Nuclear Society Spring Meeting, 2025.
- [7] T.W. Na et al., "Applicability analysis of induction bending process to P91 piping of PGSFR by high-temperature creep tests", Nuclear Engineering and Technology (Submitted), 2026.
- [8] T.W. Na et al., " Comparison of creep and stress relaxation behavior for induction bent P91 piping between structural tests and finite element analysis", Transactions of the Korean Nuclear Society Spring Meeting (In preparation), 2026.